

**Research Article**

**NUMERICAL STUDY ON TOTAL EFFICIENCY FOR SOLAR CONCENTRATING PHOTOVOLTAIC/THERMAL NANOFLUID (WATER- $\text{Al}_2\text{O}_3$ ) SYSTEM**

**\*Maifi Lyes, Kerbache Tahar, Hioual Ouided and Chari Abdelhamid**

*Physical Chemistry of Semi-Conductor Laboratory, Physics Department, Exact sciences Faculty, Constantine University, Constantine Algeria.*

*\*Author for Correspondence*

**ABSTRACT**

Hybrid thermal/photovoltaic systems associating a solar concentrator with using water- $\text{Al}_2\text{O}_3$  nanofluid as a coolant are an effective way to improve solar energy conversion yield. We present here an analysis of the effect of the mass flow rates, hydraulic diameter and concentration ratio in such a collector. A numerical simulation of the performance of the thermal/photovoltaic sensor with a heat exchanger using water- $\text{Al}_2\text{O}_3$  nanofluid as a coolant is presented. A thorough analysis of the external parameters on the efficiency and the working of a thermal/photovoltaic collector are presented. The analysis is made using the equations of the components of heat transfer cascade into a matrix of four unknown's which are the glass, cells, fluid and insulation plate temperature. This matrix is solved by the fixed point method and Gauss-Seidel, at the permanent regime. Results show that the overall conversion efficiency of the system is increasing from 22% to 72%, when mass flow rates, concentration ratio increases and hydraulic diameter decreases.

**Keywords:** *Nanofluid, Concentrator, Efficiency, Photovoltaic, Thermal*

**INTRODUCTION**

Problems of environmental pollution and energy lack in the world have become much serious recently. Solar energy as a renewable and environmentally friendly energy has the potential to meet global energy demand in the future. Methods for the conversion of solar energy can be classified into two types: a thermal option, that converts solar energy into heat, subsequently transformed into electricity, and the photovoltaic methods that converts solar energy directly into electrical energy. Therefore, there is a need to develop an ingenious method of solar energy conversion systems and then to substitute it where applications of fossil fuels are most vulnerable. One of the ingenious methods of solar energy conversion systems is the photovoltaic thermal solar collector or hybrid solar collector, which converts solar radiation directly to both thermal and electrical energies. It is very attractive for solar applications in which limited space and area related installation cost are of primary concern. The hybrid collector is also attractive when the space needed to install side-by-side solar thermal and photovoltaic collectors is not readily available.

Kern and Russel (1978) presented a prototype of a thermal/photovoltaic system using air and water as a coolant to reduce the temperature of the solar cells. A number of theoretical and experimental studies to assess the efficiency of hybrid thermal/photovoltaic system have been performed (Florschuetz, 1979; Garg and Adhikari, 1997; Garg and Adhikari, 1999; Whitfield *et al.*, 2002; Othman and Yatim, 2005; Chen *et al.*, 2008). Florschuetz (1979) used the model of hotel-Whillier to analyze the performance of the hybrid solar system that could provide domestic hot water. Garg and Adhikari (1997) have developed a stable model to simulate the performance of thermal/photovoltaic hybrid system. In the recent years much research has been reported in the literature on new solar thermal systems with lower costs. When sunlight is concentrated on the solar cell, most of the energy absorbed by the cell is converted into thermal energy which in turn increases the temperature and reduces the electrical efficiency. Therefore, it is necessary to remove heat from the cell by a heat transfer fluid (air, water...). Convective heat transfer can be enhanced passively by changing flow geometry, boundary conditions, or by enhancing thermal conductivity of the fluid. Various techniques have been proposed to enhance the heat transfer properties of fluids. Researchers have also tried to increase the thermal conductivity of base fluids by suspending micro- or larger-sized solid particles in fluids, since the thermal conductivity of solid is typically higher than that of

**Research Article**

liquids. However, due to the large size and high density of the particles, there is no good way to prevent the solid particles from settling out of suspension. The lack of stability of such suspensions induces additional flow resistance and possible erosion. Hence, fluids with dispersed coarse-grained particles have not yet been commercialized. Modern nanotechnology provides new opportunities to process and produce materials with average crystallite sizes below 50 nm. Fluids with suspended nanoparticles are called nanofluid, a term proposed in 2005 by Chon *et al.*, (2005) of the Argonne National Laboratory, USA. Nanofluids can be considered to be the next generation heat transfer fluids because they offer exciting new possibilities to enhance heat transfer performance compared to pure liquids. The aim of this study is to obtain technical to improve efficiency of hybrid thermal/photovoltaic sensor using water–Al<sub>2</sub>O<sub>3</sub> nanofluid as a coolant.

**System Model**

The hybrid thermal/photovoltaic collector considered in this work is shown in (Figure 1). The glass cover (in plastic) is inserted in order to protect the sensor against mechanical damage, the light is reflected and concentrated on the solar cell by a reflective cylindro-parabolic concentrator. The focusing system consists of the cylindro-parabolic concentrator with seven panels from (Generic 60 WP polycrystalline), with 36 cells in series. The panels are connected in series along the direction of the system; they are glued and sealed to keep surfaces cells clean. The heat exchanger bottom is covered with a good insulator to minimize heat losses to the ambient (Florschuetz 1979).

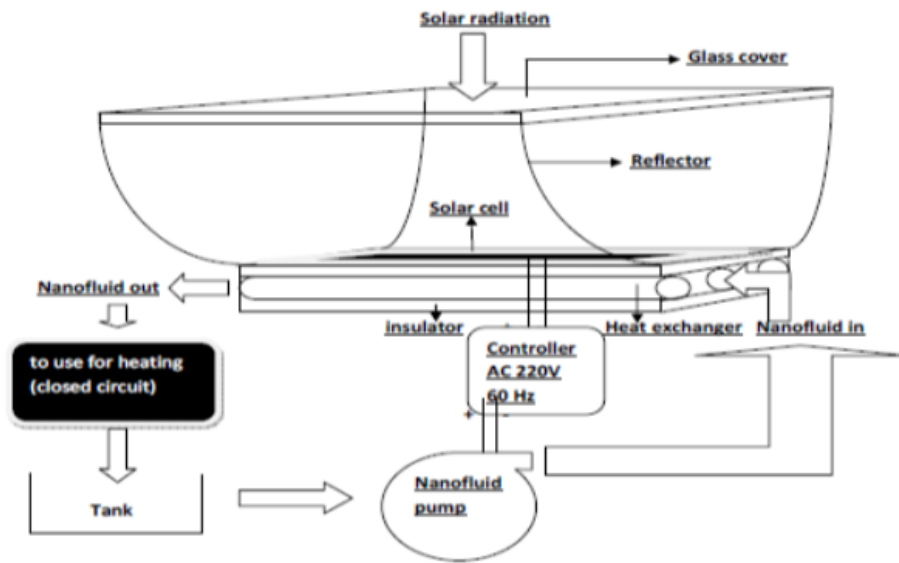


**Figure 1: The Schematic Model of Concentrating Photovoltaic/Thermal Nanofluid System**

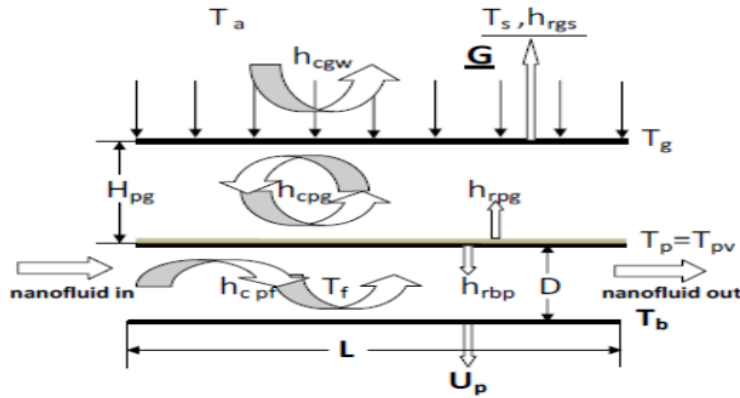
**Energy Balance**

Figure 2, shows the thermal model of the system. For the sake of simplicity, the following hypotheses are made

- A one-dimensional steady state heat transfer in the direction of the flow.
- The heat capacities of the glass, concentrator, solar cell, fins, absorber and the insulating plate are negligible.
- The parabolic concentrator is ideal and all the incident radiation in the acceptance angle can reach the solar cells.
- The solar radiation converted into thermal energy is completely absorbed by the panels and solar absorber.
- The temperature of the solar cell and the absorber are uniform.

Based on these assumptions, the equations of energy can be written as follows:

**Research Article**



**Figure 2: Thermal Model of our Thermal/Photovoltaic Sensor**

For the Glass Cover

$$w_g \phi_g C_g \frac{\partial T_g}{\partial t} + \alpha_g G C \left( 1 + \tau_g \rho_g \rho_R^{2n} \right) = h_{rgs} (T_g - T_s) + h_{cgw} (T_g - T_w) + h_{cpg} (T_g - T_p) + \frac{A_{ct}}{A_c} h_{rpg} (T_g - T_p) \quad (1)$$

Where n is the average number of reflection for radiation inside the acceptance angle. And C is the ration concentrating.

At the photovoltaic thermal plate

$$w_p \phi_p C_p \frac{\partial T_p}{\partial t} + \tau_g \alpha_p G \rho_R^n d \left( 1 + \frac{\rho_p \rho_g \rho_R^{2n}}{c} \right) (1 - P) + \tau_g \alpha_p G P \rho_R^n d \left( 1 + \frac{\rho_{pv} \rho_g \rho_R^{2n}}{c} \right) (1 - \eta_{pv}) = \frac{A_{cb}}{A_c} h_{cpf} (T_p - T_f) + \frac{A_{cb}}{A_c} h_{rpb} (T_p - T_b) + \frac{A_{ct}}{A_c} h_{cpg} (T_p - T_f) + \frac{A_{ct}}{A_c} h_{rpg} (T_p - T_g) \quad (2)$$

Where d is a correction of gap loss. P is the solar cell packing factor with Goodman *et al.*, (1976).

$\eta_p$  : is the total efficiency.

$$\eta_{pv} = \eta_{ref} \left( 1 - 0.0054 (T_p - 298.15) \right)$$

Where  $\eta_{ref}$  is a reference efficiency of solar cell at solar irradiance 1000 W/m<sup>2</sup> and temperature  $T_{ref}=25^\circ\text{C}$ . In this work  $\eta_{ref}$  is taken as 10%.

The heat exchanger

$$w_{pb} \phi_f C_f \frac{\partial T_f}{\partial t} + \frac{m_f C_f d T_f}{w_{pb} dx} = h_{cpf} (T_b - T_f) + \frac{A_{cb}}{A_c} h_{cpf} \eta_p (T_p - T_f) \quad (3)$$

Where  $m_p$  is mass flow rate (kg.s<sup>-1</sup>),  $C_f$  is specific heat (J.kg<sup>-1</sup>.k<sup>-1</sup>) and w is system width (m) (Goodman *et al.*, 1976).

The insulating plate

$$w_b \phi_b C_b \frac{\partial T_b}{\partial t} + U_b (T_b - T_a) = h_{cpf} (T_f - T_b) + \frac{A_{cb}}{A_c} h_{rpb} (T_p - T_b) \quad (4)$$

The back loss coefficient  $U_b$  is 0.0692 W.m<sup>2</sup>.k (Goodman *et al.*, 1976).

**Heat Transfer Coefficients**

In the above equations, radiative and convective heat transfer coefficients are calculated using the relations reported in reference (Ari, 1976).

The radiative heat transfer coefficients from glass cover to sky and absorber plate are taken as Ari (1976).

$$h_{rgs} = \frac{\varepsilon_g \sigma (T_g^4 - T_s^4)}{(T_g - T_a)} \quad (5)$$

Where the equivalent sky temperature is evaluated as

$$T_s = 0.0552 T_a^{1.5} \quad (6)$$

$$h_{rpg} = \frac{\sigma (T_p^2 + T_g^2) (T_p + T_g)}{\left( \frac{1}{\varepsilon_p} + \frac{1}{\varepsilon_g} - 1 \right)} \quad (7)$$

**Research Article**

$$h_{rbp} = \frac{\sigma((T_p^2+T_b^2)(T_p+T_b)}{\left(\frac{1}{\epsilon_p} + \frac{1}{\epsilon_b} - 1\right)} \tag{8}$$

The convective heat transfer coefficient of the wind is calculated by Ari (1976).

$$h_{cgw} = 2.8 + 3V_v \tag{9}$$

$V_v$  : The wind velocity is 3 m/s.

The natural convection heat transfer coefficient between the solar cells and glass cover is calculated as Zhang (2004).

$$h_{cpg} = \left(\frac{\lambda_f}{H_{pg}}\right) \left(1 + 1.44 \left(1 - \frac{1708}{R_a \cos\beta}\right) \left(1 - \frac{\sin(1.8\beta)^{1.6} 1708}{R_a \cos\beta}\right) + (R_a \cos\beta / 5830)^{\frac{1}{3}} - 1\right) \tag{10}$$

The forced convective heat transfer coefficient of cooling air is calculated by Chen *et al.*, (2008).

$$h_{cpf} = \left(\frac{\lambda_f}{D}\right) (0.0158R_e^{0.8} + (0.00181R_e + 2.92) \exp^{-\frac{0.03795X}{D}}) \tag{11}$$

Where,  $R_e$  is Reynolds number (Ari, 1976).

**Thermo Physical Properties of Nanofluid**

*Thermal Conductivity*

The thermal conductivity of the nanofluid is calculated from Chon *et al.*, (2005), which is expressed in the following form:

$$\frac{K_{nf}}{K_f} = 1 + 64.7\phi^{0.746} \left(\frac{d_f}{d_p}\right)^{0.369} \left(\frac{K_p}{K_f}\right)^{0.7476} Pr_f^{0.9955} Re_p^{1.2321} \tag{12}$$

$$Pr_f = \frac{\mu_f}{\alpha_f \rho_f}, \quad Re_p = \frac{K_p \rho_f}{3\pi \mu^2 l_f} \text{ Tand } d_p = 36.10^{-9} \text{ m}$$

Where  $k_b$  is Boltzmann number and  $l_f$  is the free average distance of water molecules that according to the suggestion of Chon *et al.*, (2005), is taken equal to 17 nm. Minsta *et al.*, (2009) approved the accuracy of the above model.

*Viscosity*

The viscosity of the nanofluid is approximated as viscosity of the base fluid  $l_f$  containing dilute suspension of fine spherical particles as given by Masoumi *et al.*, (2009).

$$\frac{\mu_{nf}}{\mu_f} = 1 + \frac{\rho_p V_b d_p^2}{72N\delta} \tag{13}$$

$$\delta = \sqrt[3]{\frac{\pi}{6\phi}} d_p, \quad V_p = \left(\frac{1}{d_p}\right) \sqrt{\frac{18K_p T}{\pi \rho_p d_p}}$$

$N = (c1\phi + c2)d_p + (c3\phi + c4)$  Is a parameter for adapting the results with experimental data where  $c1 = -1.1339 \cdot 10^{-6}$ ,  $c2 = -2.7719 \cdot 10^{-6}$ ,  $c3 = -9.09 \cdot 10^{-8}$  and  $c4 = -3.939 \cdot 10^{-7}$ .

*Density and Specific Heat*

The density and specific heat of the nanofluids are calculated by using the Pak and Cho, (1998) correlations, which are defined as follows:

$$\rho_{nf} = \phi \rho_p + (1 - \phi) \rho_f \tag{14}$$

$$(C_p)_{nf} = \frac{((1-\phi)\rho_f(C_p)_f + \phi(\rho C_p)_p)}{\rho_{nf}} \tag{15}$$

$$Pr_{nf} = \frac{\mu_{nf} C_{p,nf}}{K_{nf}} \tag{16}$$

**Method of Calculation**

We can write the equation 7 as:

$$\frac{dT_f(x)}{dx} + pT_f(x) = q \tag{17}$$

Where  $p$  and  $q$  are constants obtained by algebraic manipulations. The boundary conditions are:

$$T_f(x) = T_a, \text{ at } x$$

$$T_f(x) = T_0, \text{ at } x$$

The solution can be obtained as:

$$T_f(x) = \frac{q}{p} + \left(T_a - \frac{q}{p}\right) \exp^{-px} \tag{18}$$

**Research Article**

By grouping the four equations from equation 1 to equation 4, we obtain a four variables matrix. In the equation 18, p and q are the two unknown temperatures functions. An iterative algorithm is applied to determine these temperatures. In order to calculate the temperature of each cell of the photovoltaic concentrator, the panels is divided into  $i=252$  units of 0.031746 m length (i is also the number of series cells in the collector).  $T_o$  start the calculation, initial values at  $T_g, (T_p=T_{pv})$  and  $T_b$  are introduced. The temperature  $T_f$  of the in air flow at  $x=0$ , is equal to the ambient temperature. The new temperatures can be obtained from the matrix. Gauss-Seidel method is used to calculate the temperatures of each cell by an iterative process which is repeated until temperature values converge. Thus, the components temperatures for the first cell can be determined. Applying it as the Intel to the next cell, the components temperatures for the second cell can be similarly calculated. By repeating this step, all temperatures for the different components can be determined. Using these temperatures, one can deduce the air mass flow influence on the cells and panel efficiency.

**Performance Parameters**

Performance parameters of the hybrid sensor thermal/photovoltaic are computed as following:

The thermal efficiency of the system is:

$$\eta_{th} = \frac{\sum_{j=1}^n m_p C_f (T_{o,j} - T_{i,j})}{GC} \tag{19}$$

The electrical efficiency of the system is [10].:

$$\eta_{pv} = \frac{\sum_{j=1}^n \tau_g \alpha_{pv} G P \rho_R^n d \left( 1 + \frac{\rho_{pv} \rho_g \rho_R^{2n}}{C} \right) (\eta_{pv,j})}{GC} \tag{20}$$

The combined thermal/photovoltaic efficiency is the sum of photovoltaic and thermal efficiencies of the system.

$$\eta_{tot} = \eta_{pv} + \eta_t - \eta_c \tag{21}$$

$\eta_c$ : Efficiency of pump

**RESULTS AND DISCUSSION**

**Results**

Some main thermo-physical parameters used in the calculation are presented in Table 1. In practice, time variation of the enthalpy of the captor’s components, namely the  $(w \phi C \frac{\partial T}{\partial t})$  terms are negligible (Kadri *et al.*, 2012). The operating conditions for the calculated photovoltaic thermal nanofluid system are: the wind velocity is 3m/s and the solar radiation is 800 w/m<sup>2</sup>.

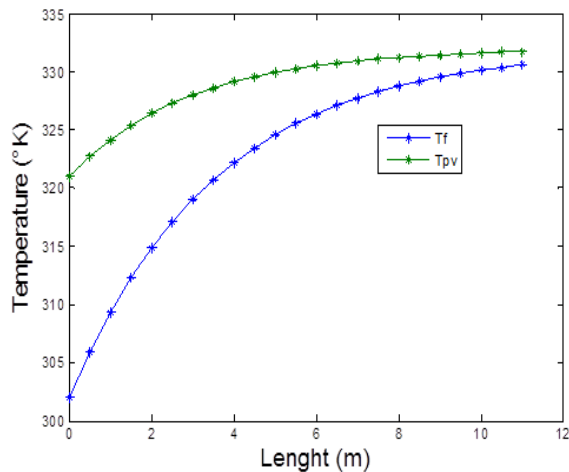


**Figure 3: Variation of Temperature of System along the Length Direction**

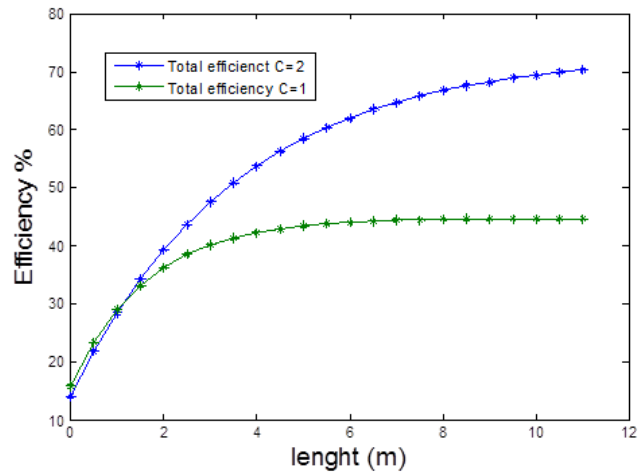


**Figure 4: Variation of Total Efficiency with and without Concentrating**

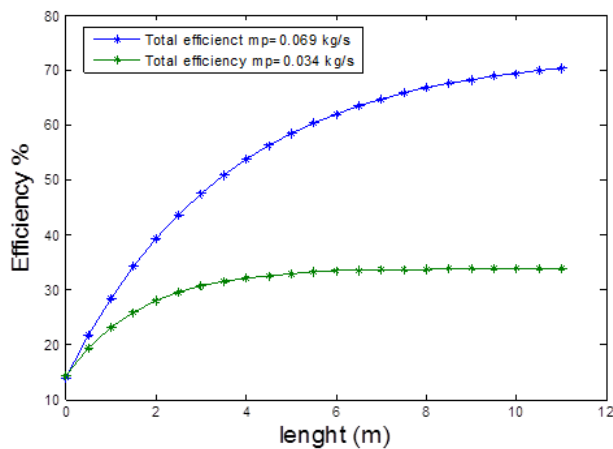
**Research Article**

**Table 1: Thermo-Physical and Internal Parameters of the System Photovoltaic Panels**

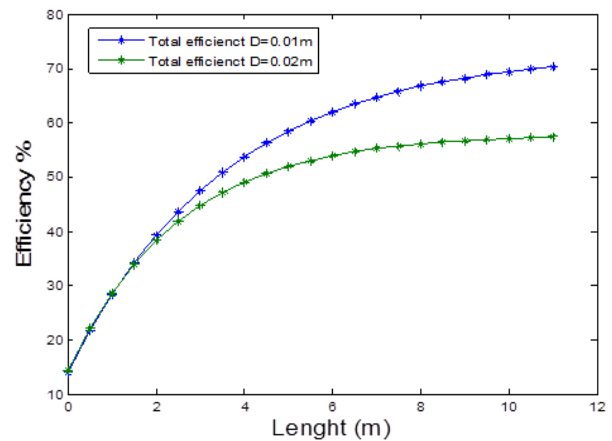
Parameter	Value	Parameter	Value	Parameter	Value
$\alpha$	0.04	d	0.95	$C_{AL2O3}$	900 $JKg^{-1}K^{-1}$
$\alpha$	0.95	p	0.52	$\rho_{water}$	997.1 $Kg/m^3$
$\alpha$	0.9	$\epsilon_i$	0.86	$\rho_{AL2O3}$	3.97 $Kg/m^3$
$\tau_i$	0.9	$\epsilon_i$	0.95	$K_{water}$	0.613 $w/m^{\circ}K$
$\rho$	0.06	$\epsilon_i$	0.95	$K_{AL2O3}$	180 $w/m^{\circ}K$
$\rho$	0.94	$\sigma$	$5.66.10^{-8} Wm^{-2}k^{-4}$	$\phi$	3%
$\rho$	0.05	$U_p$	0.5 $Wm^{-2}k^{-1}$	n	0.61
$\rho$	0.05	$C_{water}$	4.2 $JKg^{-1}K^{-1}$	C	2

Figure 3 shows the temperature variation of the nanofluid and cell solar along the length of the system with and irradiation solar is the case of  $G=800 w/m^2$  and  $m_p=0.069 Kg/s$ . It is obvious that the temperatures increase along the length of the system, and the solar cell temperature is higher than the fluid temperature.

The nanofluid stream temperature increases quickly at the inlet region but slowly at the outlet region, the temperature difference between the solar cell and the nanofluid stream decreases with increasing in the length of system. Under the same operating conditions, Figure 4 presents the variations of the total efficiency of the system with and without truncated concentrator cylindro-parabolic in the length direction. It can be seen that the total efficiency increase along the length direction. The total efficiency of the system with concentrator cylindro-parabolic is almost 72% which is close the value obtained by Othman *et al.*, (1997).



**Figure 5: Variation of Total Efficiency System with Different Nanofluid Mass Flow Rate**



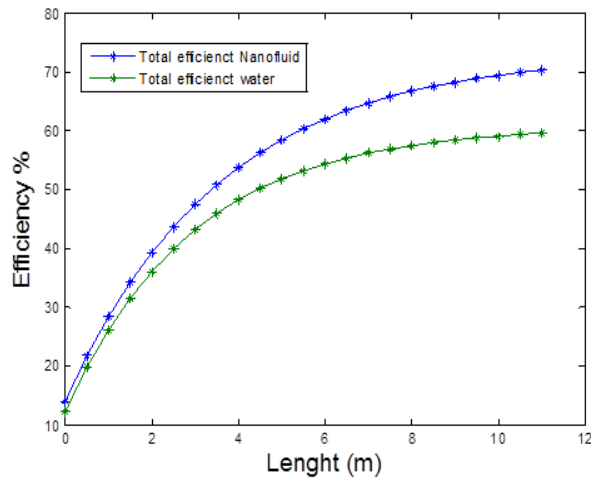
**Figure 6: Variation of Total Efficiency with Different Hydraulic Diameter**

The figure 5 presents the effect of the mass flow rates of nanofluid on the total efficiency along the length of the system. It can be observed that the total efficiency increases with the increase of the mass flow rates.

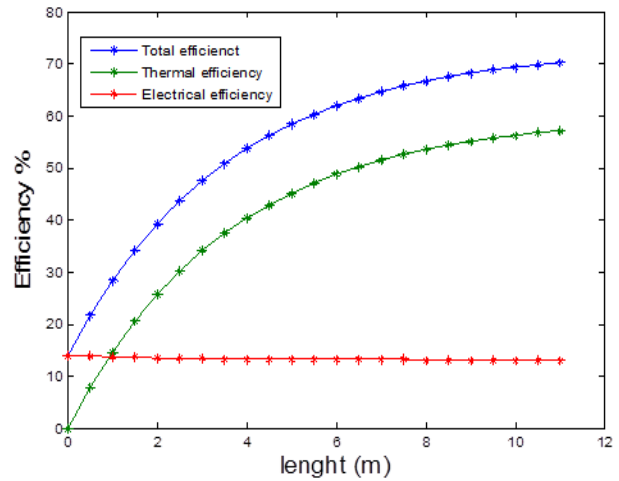
Decreasing of the hydraulic diameter Figure 6 will increase of the nanofluid mass flow, will decrease the temperature of the system, thereby reducing the heat loss from the system to the ambient. This will increase the efficiency of the system.

Figure 7 shows the efficiency difference between the nanofluid and water increases slowly at the inlet region but quickly at the outlet region. Under the same operating conditions, the total efficiency of the nanofluid is the 72% is higher than that of the total efficiency of the water fluid 60%.

**Research Article**



**Figure 7: Variation of Total Efficiency System with Different Fluid**



**Figure 8: Variation of Total Thermal Electrical Efficiency along the Length Direction**

**Conclusion**

The electrical thermal efficiency of the photovoltaic thermal nanofluid system with concentrator cylindro-parabolic are simulated. The main conclusions are as follows.

The temperatures of the solar cell and nanofluid increase along the length of the system, and the temperature of cell solar is higher than others. The temperatures of the nanofluid and cell solar with concentrator cylindro-parabolic are higher than those without concentrator. The total efficiency of the system increase with increasing of system length, but the electrical efficiency decreases Figure 8. The total efficiency of the system with concentrator cylindro-parabolic is almost 72%. The total efficiency of the system increase with the increasing of the fluid mass flow rate, and decrease with the increasing of the hydraulic diameter. The total efficiency of the nanofluid is higher than that of the total efficiency of the water.

**Nomenclature**

A	Area	m <sup>2</sup>
E	Electrical energy	W
D	hydraulic diameter	m
G	Solar radiation	W.m <sup>-2</sup>
h	heat transfer coefficient	W.m <sup>-2</sup> .K <sup>-1</sup>
H	Height	m
L	length	m
V	velocity	m.s <sup>-1</sup>
m	Mass flow rate	kg.s <sup>-1</sup> m <sup>-2</sup>
Q	energy	W
Ra	Rayleigh number	/
Re	Reynolds number	/
T	Temperature	°K
w	thickness	m
x	Direction variable	m

**Greek Letters**

$\alpha$	Absorptivity	
$\beta$	Acceptance angle	°
$\eta$	efficiency	
$\tau$	Transmitivity	

**Research Article**

$\rho$	reflectivity	
$\rho_R$	reflector	
$\lambda$	Thermal conductivity	$W \cdot m \cdot K^{-1}$
$\delta$	Thickness	m
$\varepsilon$	Emissivity	
$\varphi$	density	$Kg \cdot m^{-3}$
$\sigma$	Boltzmann number	$W \cdot m^{-2} \cdot K^{-4}$

**Subscripts**

a	Ambient
b	Back pate
c	Convective
cb	Top surface of absorber plate
ct	Bottom surface of absorber plate
g	glass
f	fluid
i	inlet
o	outlet
p	Absorber plate
pv	Solar cell
r	radiative
s	sky
th	thermal
w	Ambient/ wind

**REFERENCES**

- Ari R (1976).** Optical and thermal properties of compound parabolic concentrators. *Solar Energy* **18** 497-511.
- Chen X, Xuan YM and Han YG (2008).** Investigation on performance of a solar thermophotovoltaic system. *Science in China, Series E: Technological Sciences* **51** 2285-2294.
- Chon CH, Kihm KD, Lee SP and Choi SUS (2005).** Empirical correlation finding the role of temperature and particle size for nanofluid (Al<sub>2</sub>O<sub>3</sub>) thermal conductivity enhancement. *Applied Physics Letters* **87** 153107–153110.
- Donatien N (1998).** Thermal behavior of a combined plastic-glass flat plate solar air collector. *Revue Générale de Thermique* **37** 973-980.
- Florschuetz LW (1979).** Extension of the Hottel-Whillier model to the analysis of combined photovoltaic thermal flat collector. *Solar Energy* **22** 361-366.
- Garg HP and Adhikari RS (1997).** Conventional hybrid photovoltaic thermal (PV/T) air heating collectors: Steady-state simulation. *Renewable Energy* **11** 363-385.
- Garg HP and Adhikari RS (1999).** Performance analysis of a hybrid photovoltaic /thermal (PV/T) collector with integrated CPC troughs. *International Journal of Energy Research* **23** 1295-1304.
- Goodman NB, Rabl A and Winston R (1976).** Optical and thermal design considerations for ideal light collectors. *Sharing the Sun* **2** 336-350.
- Kadri R, Andrei H, Gaubert JP, Ivanovici T, Champenois G and Andrei P (2012).** Modeling of the Photovoltaic Cell Circuit Parameters for Optimum Connection Model and Real-Time Emulator with Partial Shadow Conditions. *Energy* **42** 57-67.
- Kern EC and Russel MC (1978).** Combined photovoltaic and thermal hybrid collector system. *Proceedings of 13th IEEE Photovoltaic Specialists Conference* 1153-1157.
- Masoumi N, Sohrabi AN and Behzadmehr A (2009).** New model for calculating the effective viscosity of nanofluids. *Journal of Physics D: Applied Physics* **42** 055501–055506.



**Research Article**

**Mintsa HA, Roy G, Nguyen CT and Doucet D (2009).** New temperature dependent thermal conductivity data for water-based nanofluids. *International Journal of Thermal Sciences* **48** 363–371.

**Othman MW and Yatim B (2005).** Performance analysis of a double-pass photovoltaic /thermal (PV/T) solar collector with CPC and fins. *Renewable Energy* **30** 2005-2017.

**Pak BC and Cho YI (1998).** Hydrodynamic and heat transfer study of dispersed fluids with submicron metallic oxide particles. *Experimental Heat Transfer* **11** 151–170.

**Ramos H, Campayo Martín JA, Zamora Belver JJ, Larrañaga Lesaka I, Zulueta J, Guerrero E and Puelles Pérez E (2010).** Modelling of Photovoltaic Module. *Conference on Renewable Energies and Power Quality (ICREPQ'10)* Granada (Spain).

**Sopian K, Liu HT, Kakac S and Veziroglu TN (2000).** Performance of a double pass photovoltaic thermal solar collector suitable for solar drying systems. *Energy Conversion and Management* **41** 353-365.

**Walker G (2001).** Evaluating MPPT converter topologies using a MATLAB PV model. *Journal of Electrical and Electronic Engineering* **21** 49–56.

**Whitfield GR, Bentley RW, Weatherby CK and Clive B (2002).** The development of small concentrating pv systems. *Proceedings of 29th IEEE Photovoltaic Specialists Conference*, New Orleans, 1377-1379.

**Zhang HF (2004).** *Utilization Principle and Computer Simulation of Solar Energy (in Chinese)*, 2nd edition, (China, Xian: Xian Northwestern Polytechnic University Press).